Proceedings of the
Annual Stability Conference
Structural Stability Research Council
St. Louis, Missouri, April 2-5, 2019

Moment gradient factors for singly-symmetric I-sections

Matthew C. Reichenbach[1], Yangqing Liu[2], Todd A. Helwig[3], Michael D. Engelhardt[4]

Abstract
The lateral-torsional buckling behavior of singly-symmetric I-sections can be complicated due to significant variations in the sizes of the flanges. In many situations, the section is nonprismatic, which further complicates the lateral-torsional buckling behavior. There are substantial differences in the moment gradient factors in the AISC and AASHTO design specification. The AASHTO expression is relatively complicated to apply for realistic problems. This paper focuses on a parametric finite element study on the buckling behavior of singly-symmetric I-sections subjected to moment gradient. The study includes the effects of moment gradient on both prismatic and nonprismatic sections. Expressions in the commentary of the AISC specification are examined for application in bridge girders. Design recommendations are made for evaluating the lateral-torsional buckling behavior in both the positive and negative moment regions.

1. Introduction

Lateral-torsional buckling (LTB) is a complex limit state that often governs the design of steel I-girders. LTB is especially critical during construction when bracing on a noncomposite beam may be limited and/or the concrete deck has not cured. Without adequate bracing during erection and deck casting, the girders can buckle. In addition, questions often arise about stability in the negative moment region of composite girders in the final constructed state.

To further complicate the LTB behavior, I-girders in bridge applications are often: (1) designed as singly-symmetric (or monosymmetric), (2) designed as nonprismatic, and (3) subjected to moment gradients. Due to composite action with the concrete deck, girder sections can be singly-symmetric and have a smaller top flange relative to the bottom flange. The relative difference between the flange sizes is characterized by the degree of monosymmetry, ρ, which is the ratio of weak-axis moment of inertia of the compression flange to the weak-axis moment of inertia of the entire cross-section.

Engineers often transition flanges and webs at discrete locations along the length of the span to accommodate variations in stress and to provide a more economical and efficient design.

[1] Graduate Research Assistant, The University of Texas at Austin, <reichenbach.matt@utexas.edu>
[2] Visiting Scholar at UT Austin, Tongji University, < 1432232@tongji.edu.cn >
[3] Professor, The University of Texas at Austin, <thelwig@ mail.utexas.edu >
[4] Professor, The University of Texas at Austin, <mde@mail.utexas.edu>

Transitions on these nonprismatic beams can include any combination of increased plate thicknesses and/or widths. Estimating the LTB resistance of a singly-symmetric, nonprismatic beam subjected to moment gradient can be challenging.

Current AASHTO (2016) and AISC (2017) specifications simplify the design procedure by making use of approximate solutions for estimating the LTB resistance of singly-symmetric beams. Despite being developed specifically for doubly-symmetric sections, these simplified equations provide accurate approximations of the exact solution. White and Jung (2003) found that the simplified design equations generally provide solutions within 12% of the exact solution for typical singly-symmetric sections but produce larger disparities for extreme monosymmetric sections. The exact solution for LTB of singly-symmetric sections under uniform moment is available in the literature (Galambos 1968, Ziemian 2010) and is given in the following expression:

$$M_{cr} = \frac{\pi^2 E I_y}{L_b^2}\left\{\frac{\beta_x}{2} + \sqrt{\left(\frac{\beta_x}{2}\right)^2 + \left[\frac{C_w}{I_y} + \frac{GJ}{EI_y}\frac{L_b^2}{\pi^2}\right]}\right\} \quad (1)$$

where E is the modulus of elasticity, I_y is the weak-axis moment of inertia of the section, L_b is unbraced length of the beam segment, C_w is warping constant of the section, G is the elastic shear modulus, J is the St. Venant torsional constant of the section, and β_x is a coefficient of monosymmetry, which is defined Ziemian (2010).

Previous studies have primarily focused on the LTB behavior of singly-symmetric, prismatic sections including the impacts of moment gradient and load position (Helwig et al. 1997). The effects of nonprismatic sections on LTB, however, have been a less-researched problem; consequently, current AASHTO Specifications employ a conservative approach for estimating LTB resistance of nonprismatic girders in Section 6.10.8.2.3. Other than a few exceptions, AASHTO recommends using the smallest resistance to characterize the entire nonprismatic unbraced segment.

Additionally, moment gradient effects on the LTB behavior have traditionally been considered with the use of a moment gradient factor (C_b). Most design specifications make use of buckling solutions that were developed for uniform moment loading, including Eq. 1 above. The C_b factor then amplifies the LTB resistance with respect to the uniform moment case.

The C_b expression in AASHTO Section 6.10.8.2.3 is based upon a long-standing equation that was applicable to beams with no loading between the brace points. Since all sections have loading between the brace points (i.e. self-weight), such a solution is not practical. As a result, the AASHTO expression includes a number of conservative exceptions to make the expression applicable for general use; the expression can also be cumbersome to calculate and implement.

In contrast, the commentary of the AISC Specification provides an expression for the moment gradient factor that is generally simpler to apply and provides reasonable estimates of the buckling behavior. For singly-symmetric beams subjected to reverse-curvature bending, a special term R_m is added to the standard AISC C_b expression. The equation in full is presented below:

$$C_b = \left[\frac{12.5M_{max}}{2.5M_{max}+3M_A+4M_B+3M_C}\right]\left(0.5+2\left(\frac{I_{yt}}{I_y}\right)^2\right) \leq 3.0 \quad (2)$$

where M_{max} is the absolute value of the maximum moment in the unbraced segment, M_A, M_B, M_C are the absolute value of the quarter-point, midpoint, and three-quarter-point moment in the unbraced segment, respectively, and I_{yt}/I_y (or ρ_{top}) is the degree of monosymmetry with respect to the top flange. The term outside of the square brackets is referred to as R_m in the AISC Specification. For single curvature bending, R_m is taken as 1.0. The expression for C_b is capped at 3.0, which takes effect for high values of ρ_{top} (i.e. a much larger top flange than bottom flange).

With that in mind, the intent of this paper is to examine the AISC C_b expression for common design conditions that occur in steel bridge applications, specifically the effects of nonprismatic sections. Through a parametric finite element study, the effects of varying span lengths, span configurations, intermediate bracing schemes, monosymmetry, flange transitions, and moment gradients are investigated and quantified with respect to the AISC C_b expression. Only midheight loading application and uniformly distributed loads are considered in the study. In general, this paper focuses on only the most common cases for each of these variables, and the results are intended to cover the majority of singly-symmetric, nonprismatic sections found in practice.

Following this introduction, an overview of the variables considered in the parametric studies is provided along with a discussion of the procedures used to conduct the finite element analysis (FEA). Select results from the parametric studies are then presented and compared to the AISC Commentary equation for C_b. Based on the findings of the parametric studies, design recommendations are made for evaluating the LTB behavior of singly-symmetric and nonprismatic I-girders in both the positive and negative moment regions.

2. Variables Considered in Parametric Study

The following variables were investigated in the parametric FEA study: (1) span-to-depth ratio and intermediate bracing schemes, (2) moment gradients and span configurations, (3) degrees of monosymmetry, and (4) nonprismatic sections and flange transitions. A matrix was developed to address only practical combinations of these key variables. This paper does not study extreme cases but rather focuses on systems that fall into practical ranges encountered in design. The following subsections provide a brief overview of each variable.

2.1 Span-to-Depth Ratio and Intermediate Bracing

Span-to-depth ratios of 15, 20, and 25 were considered. These values represent common practice for bridge girders. Within each of the different span-to-depth ratios, different bracing schemes were evaluated for their effect on the LTB behavior. Braces only at the ends ($L_b = L$) and intermediate bracing schemes of one-half ($L_b = L/2$) and one-third ($L_b = L/3$) of the span length were considered, which produced unbraced length-to-depth ratios of {7.5, 10, 12.5} and {5, 6.67, 8.33}, respectively. The cases with larger unbraced lengths are representative of steel girders during the erection process, and cases with smaller brace spacing represent girders during deck casting and in the final constructed state.

2.2 Moment Gradient and Span Configuration

With consideration of the various bracing schemes, nine different moment gradients along with

the uniform moment case were evaluated. These nine cases were considered the most representative for bridges throughout the construction and service life. Fig. 1 presents these cases graphically. An important aspect to understand is that when several braces are introduced, moment gradient effects are much less pronounced and the C_b factor tends to unity. As a result, cases with four or more braces are of less interest and are not considered in the study.

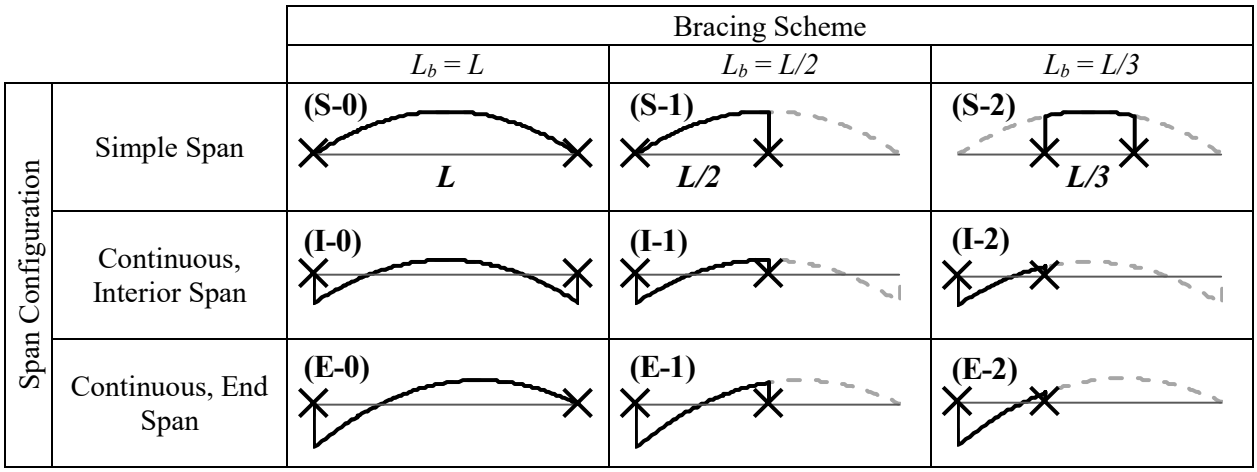

Figure 1: Moment gradients considered in the parametric study

As illustrated in Fig. 1, the nine moment gradient cases categorize girder types into three span configurations: (1) simply-supported single span, (2) interior span of a continuous unit, and (3) end span of a continuous unit. Both single-curvature and reverse-curvature bending cases are included. These three conditions, aside from a cantilever or overhang condition often observed during erection, represent the most common span arrangements and support conditions for steel I-girder bridges.

As indicated by the moment diagrams in Fig. 1, only uniformly distributed loads are considered. During construction, the major transverse loads on girders are uniformly distributed (self-weight of steel and wet concrete), and substantial concentrated loads are seldom applied. In the final constructed stage, bridge girders are typically designed for a moment envelope, which generally follow shapes similar to the diagrams in Fig. 1. As such, point load moment gradients were considered less important for bridge applications and were thus not included in the parametric study. The recommendations in the paper will still likely have applications for moment gradients caused by concentrated forces; however, this study focused on the most common conditions facing designers.

Moment gradients are abbreviated in this paper with an alphanumeric identifier, where the letter signifies the span configuration (S for simple span, I for interior span, E for end span) and the number signifies the number of intermediate braces (0 for zero intermediate braces, 1 for one intermediate brace, 2 for two intermediate braces).

With these factors in mind, it is important to highlight where each of these simple moment gradients would occur during the construction and service life of a bridge. Cases S-0, I-0, and E-0, in which no intermediate braces are used, represent worst-case conditions during steel erection where self-weight is the primary loading. Since bracing will often be introduced once two or more

girders are erected in a span, these cases specifically represent the first girder erected in a span.

The corresponding cases with one or two intermediate braces largely represent a girder during deck casting or in its final constructed state, but only the more critical unbraced segments were considered. For example, cases I-2 and E-2 are especially important for evaluating the negative moment region of a composite girder. In summary, the nine moment gradient cases considered are not exhaustive but encompass the common loading conditions that are likely critical for girder stability.

2.3 Degree of Monosymmetry

The parametric study was conducted with degrees of monosymmetry, ρ, ranging from 0.1 to 0.9. Sections that do not satisfy $0.1 \leq \rho \leq 0.9$ are essentially T-sections, for which the LTB is difficult to predict computationally due to web distortion and local buckling. As such, sections outside of this range were not included in this study. Given that both single-curvature and reverse-curvature bending cases are evaluated and that the compression flange may change between the top and bottom flanges along the unbraced length, the degree of monosymmetry with respect to the top flange is the adopted notation herein. As such, ρ_{top} is defined as the ratio between the weak-axis moment of inertia of the top flange and the weak-axis moment of inertia of the entire section:

$$\rho_{top} = \frac{I_{yt}}{I_y} \tag{3}$$

For practical bridge applications, ρ_{top} ranges from 0.2 to 0.5, for which the size of the top flange is smaller than or equal to the size of the bottom flange. Although results for ρ_{top} values outside of the practical range are presented in this paper for completeness, the primary focus of the conclusions is for sections where $0.2 \leq \rho_{top} \leq 0.5$.

In order to streamline the parametric studies, the distance between the flange centroids was maintained at a constant 60 inches, and the web thickness was fixed at 7/8 of an inch. For all cases, the web satisfied the noncompact web slenderness limits as a means to safeguard against web distortion and local buckling. The various ρ_{top} values were then achieved by adjusting the width and thickness of the top and bottom flanges. Flange width-to-thickness ratios were selected to satisfy slenderness and proportion limits established in AASHTO Section 6.10.2.2. Fig. 2 depicts a typical cross-section used in the computational studies for $\rho_{top} \leq 0.5$. Note that sections with $\rho_{top} \geq 0.5$ are similar to its counterpart for $\rho_{top} \leq 0.5$, except that the flanges are flipped.

For nonprismatic beams, the ρ_{top} value may not be uniform along the unbraced length. For the sake of clarity, the ρ_{top} values reported in subsequent results correspond to the monosymmetry of the small cross-section, or the base section, which is identified as $\rho_{top,base}$.

2.4 Nonprismatic Sections

A major focus of the investigation was to evaluate the effects of a nonprismatic section on the LTB behavior of an unbraced girder segment. In particular, variations in flange thickness have been considered. Similar to the other variables, only common cases for flange transitions were included in the parametric study. To simplify the computations, all transitions were assumed to occur at $0.3L$ and $0.7L$ of the full span, as demonstrated by Fig. 3. For the simple span condition, flange

transitions were considered near the middle of the beam; for the continuous span cases, transitions were considered in the negative moment regions. This is consistent with common bridge engineering practice.

For each case outlined above, only the thickness of the flanges was increased within the transition region; the flange width was held constant. The increase in flange thickness is described as a multiplier to the weak-axis moment of inertia (I_{yt} or I_{yb}) of the base, smaller section. In other words, I_{yt} multiplier = I_{yb} multiplier = 1 represents a prismatic beam. I_y multipliers included 1, 1.25, 1.5, and 1.75. As an example, a specific case is depicted in Fig. 2, which illustrates the plate thicknesses used to develop the nonprismatic girder for the simple span case (S) with I_{yt} and I_{yb} multipliers of 1 and 1.5, respectively. All combinations of these parameters are then illustrated in Fig. 3.

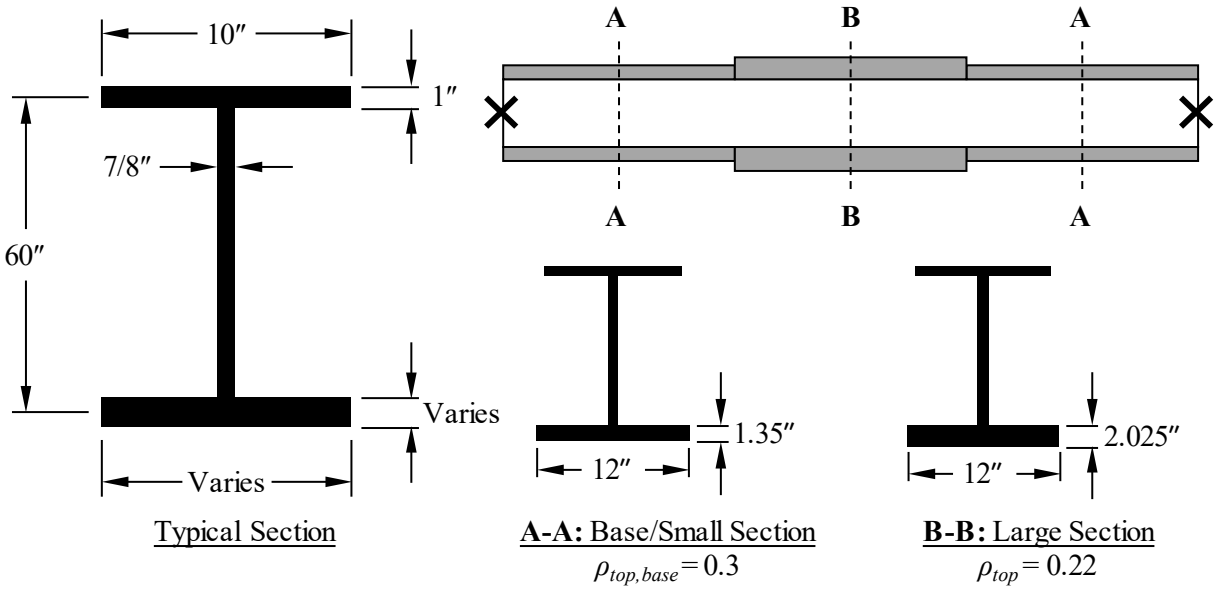

Figure 2: Typical cross-section used in the parametric study and an example showing how a simply-supported nonprismatic girder with flange transitions is developed

Note that a case in which the top flange multiplier exceeds the bottom flange multiplier was not considered, as this is uncommon in bridge engineering practice. The I_{yt} value was therefore either equal to or less than the I_{yb} value for all cases. By varying the bottom flange thickness relative to the top flange thickness, it is apparent that the ρ_{top} is no longer constant along an unbraced length, as shown in the example in Fig. 2.

The flange transitions shown in Fig. 3 were also maintained for the single intermediate bracing scheme. No flange transitions were considered for the two-intermediate bracing scheme given the close proximity of $L/3$ and $0.3L$. To clarify, an example of this is presented in Fig. 4 for the simple span cases (S-0, S-1, and S-2). A similar layout is considered for the continuous, interior span and continuous, end span cases.

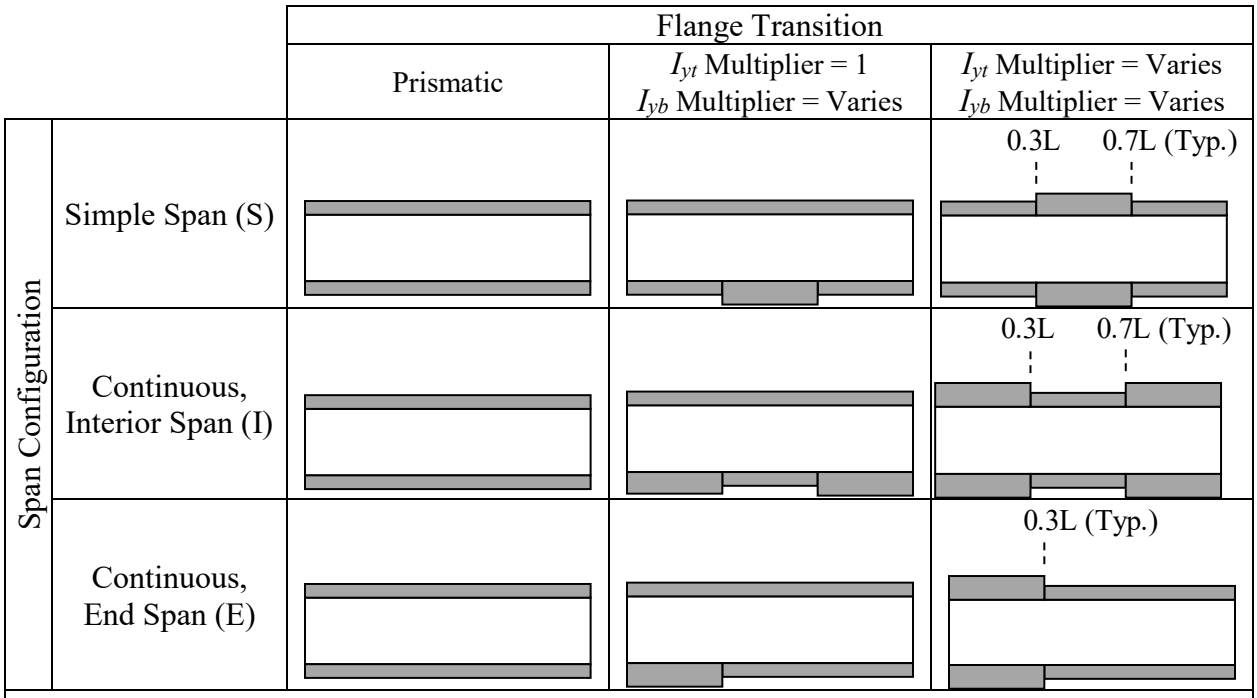

Figure 3: Flange transitions considered in the parametric study

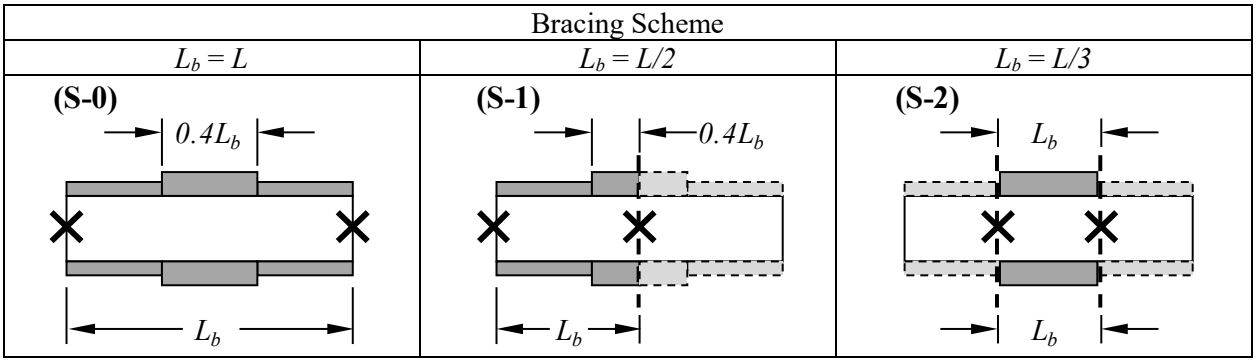

Figure 4: Flange transition cases for simply-supported condition with different intermediate bracing schemes

3. Finite Element Model

The finite element software Abaqus (2017) was used to conduct the parametric studies outlined above. Eigenvalue buckling analyses were conducted to determine bifurcation loads and therefore critical buckling moments. Cross-sections of the girders were modeled with shell elements, and transverse stiffeners were included to eliminate any potential for local buckling or web distortion that may affect the LTB response. Brace points were represented by simple torsional support conditions, in which the top and bottom flange-to-web junctions were restrained against out-of-plane translation. Though, the cross sections were still free to warp.

Specific moment gradients and intermediate bracing schemes were achieved in Abaqus by modeling only the unbraced segment of interest. Thus, the warping restraint and contributions from adjacent, unbraced segments were conservatively neglected in the FEA models, which is consistent with general design specifications. By only modeling the critical unbraced segment, the moment

gradients were achieved with a combination of a uniformly distributed transverse load and end moments, which were represented as effective line loads on the top and bottom flanges. An example of the applied loading for cases S-0, S-1, and S-2 is demonstrated in Fig. 5. This method of modeling is consistent with the loading conditions utilized in Helwig et al. (1997).

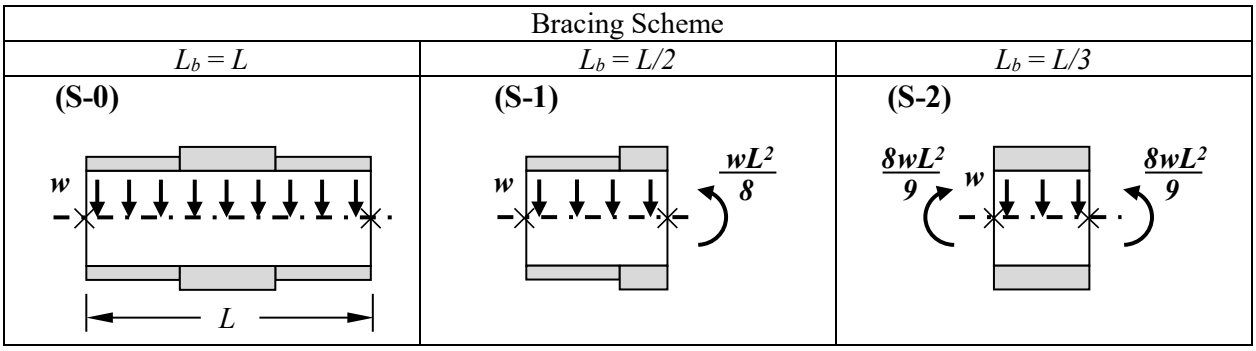

Figure 5: Applied loading scheme for simply-supported condition with different intermediate bracing schemes

4. Results and Comparisons to AISC C_b Expression

Nonprismatic sections have been shown to affect the LTB behavior of beams with respect to both moment gradient factors and the accuracy of the Eq. 1 and similar design expressions; however, the focus of this paper is quantifying the effects of flange transitions on traditional C_b factors.

C_b factors are derived computationally by comparing the critical buckling load corresponding to uniform moment along an unbraced segment to the critical buckling load corresponding to a moment gradient along the same segment. In order to determine the finite element solution for C_b, two eigenvalue buckling analyses were carried out: (1) the beam with moment gradient ($M_{cr\,FEA,MG}$) and (2) the beam with uniform moment ($M_{cr\,FEA,UM}$). This expression is shown in Eq. 4:

$$C_{b,FEA} = \frac{M_{cr\,FEA,MG}}{M_{cr,\,FEA,UM}} \tag{4}$$

Note that the subscript, FEA, is added to emphasize that they are based on finite element results and to differentiate them from the theoretical solution in Eq. 1. For prismatic sections in single-curvature bending, $C_{b,FEA}$ need only be checked at the location of maximum moment in the compression flange. For singly-symmetric, nonprismatic sections with reverse-curvature bending, the calculation of $C_{b,FEA}$ involves several checks. The moments corresponding to the critical buckling load in all unique compression flanges were checked against the uniform moment case.

This section of the paper investigates moment gradient effects by comparing FEA results for uniform moment and FEA results for various moment gradients. Critical buckling loads were obtained from the Abaqus output, and the analytical solutions for $M_{cr,FEA,MG}$ and $M_{cr,FEA,UM}$ are compared to Eq. 2, the AISC design equation for estimating C_b.

This procedure was performed for all variables in the parametric study. For brevity, only representative examples are presented in this paper. The variables considered were previously outlined in Section 2 of this paper. One of those variables, span-to-depth ratio, has a relatively small influence on the $C_{b,FEA}$, as shown in Fig. 6.

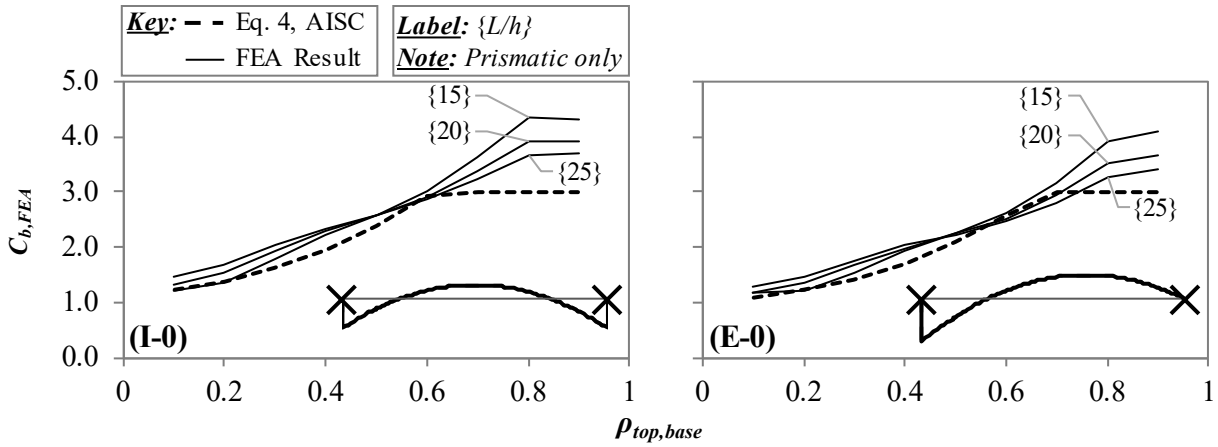

Figure 6: FEA results compared to the AISC approximate solution (Eq. 2) for various span-to-depth ratios and moment gradient cases I-0 and E-0.

Fig. 6 shows the FEA-based results for $C_{b,FEA}$ ($M_{cr,FEA,MG}$ / $M_{cr,FEA,UM}$) compared to the AISC design equation (Eq. 2) for two sample moment gradient cases, I-0 and E-0. Only the results for prismatic beams are presented. This data demonstrates that the $C_{b,FEA}$ varies slightly with the L/h ratio, especially for $\rho_{top,base} > 0.5$. For $\rho_{top,base} < 0.5$, girders with $L/h = 15$ result in lower moment gradient factors than girders with $L/h = 25$. Unless noted otherwise, the remainder of the figures in this paper will set L/h at 15, given that it is most critical for practical values of $\rho_{top,base}$.

Fig. 7 and Fig. 8 present the FEA-based C_b results for various flange transitions, intermediate bracing schemes, $\rho_{top,base}$ values, and moment gradients. Fig. 7 displays the results for cases with zero and one intermediate brace, whereas Fig. 8 displays the results for cases with two intermediate braces. Within each of the flange transitions considered, several I_y multiplier cases {I_{yt} multiplier, I_{yb} multiplier} are plotted in the figures: prismatic beam segment {1,1}, nonprismatic segment with only the bottom flange increasing {1,1.5}, nonprismatic segment with both flanges increasing {1.5,1.5}. The remainder of the cases are similar but are not presented in this paper. As stated earlier, the cases with two intermediate braces do not consider a flange transition since the transition was so close to the end.

For case S-0, Eq. 2 approximates the moment gradient factor $C_{b,FEA}$ well for all variations of I_{yt} and I_{yb} multipliers. In fact, the AISC equation provides more conservative estimates for nonprismatic girder segments than for prismatic segments. A similar observation is made for moment gradient S-1, for which one intermediate brace is added.

For case I-0, the AISC equation provides a reasonable estimate for $C_{b,FEA}$ when $\rho_{top,base} \leq 0.5$ for all cases shown and conservative estimates for $\rho_{top,base} > 0.8$; however, the C_b values are higher than 3.0 in that region. Note that the ratio of the yield moment to M_{cr} is typically in the range of 3-5 for smaller unbraced lengths, so the conservatism has no impact on practical problems since the limit state of yielding will control over LTB. However, the approximate solution is slightly unconservative for $\rho_{top,base}$ values around 0.6, especially for nonprismatic girders, but is still within 5% of the FEA solution. When an intermediate brace is added and the moment gradient case I-1 is evaluated, the AISC equation is about 10-30% conservative for practical $\rho_{top,base}$ values of 0.2 to 0.5 for nonprismatic sections.

Results for moment gradient cases E-0 and E-1 are similar to the results of I-0 and I-1, given that the end moments are similar. For case E-1, the AISC equation provides a moment gradient factor that is 30-40% conservative for $\rho_{top,base}$ values of 0.2 to 0.5.

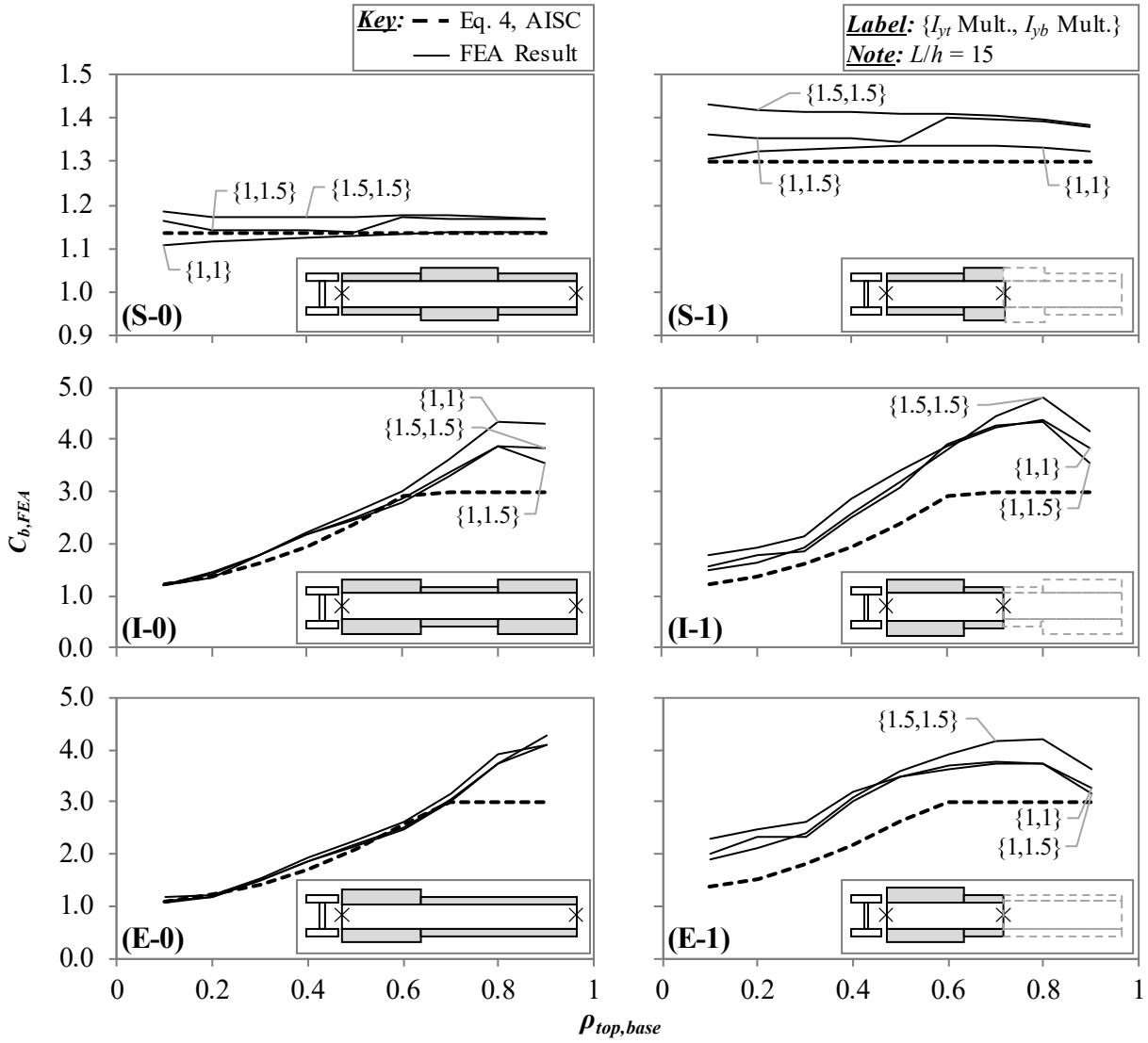

Figure 7: FEA results compared to the AISC approximate solution (Eq. 2) for various flange transition schemes and moment gradient cases S-0, S-1, I-0, I-1, E-0, and E-1.

From Fig. 8, it is apparent that the AISC equation provides an accurate estimate of $C_{b,FEA}$ for moment gradient case S-2. The $C_{b,FEA}$ values approach unity given that the moment gradient is close to the uniform moment conditions. For cases I-2 and E-2, the moment gradient is nearly linear and includes a small portion of reverse-curvature bending. The bottom flange is primarily in compression except for the right end of the unbraced length. The inflection point is within $0.33L_b$ and $0.25L_b$ of the nearest brace point for these two cases, respectively; or in other words, the ratio of the smaller end moment to the larger end moment (M_{small}/M_{large}) is -0.33 and -0.22, respectively. In contrast, the respective inflection points in cases I-1 and E-1 are within $0.44L_b$ and $0.5L_b$ of the nearest brace point, and the M_{small}/M_{large} ratios are -0.5 for both cases.

The R_m factor in Eq. 2 is limited in that it becomes an active term for any and all reverse-curvature bending, even for cases in which the inflection point is close to the brace point and moment is relatively small at the end closest to the inflection point. Because of this, Eq. 2 provides poor approximations for these special cases due to the inclusion of the R_m term. Instead, better estimates for $C_{b,FEA}$ are provided when the R_m term is neglected. Note that similar observations are made when the moment diagrams are flipped, and the top flange is primarily in compression. For cases I-2 and E-2, Fig. 8 compares the analytical solution with two forms of Eq. 2: (1) with the R_m term and (2) without the R_m term.

It is evident that, when the R_m term is included, Eq. 2 is relatively conservative for $\rho_{top,base} < 0.5$ and potentially unconservative for $\rho_{top,base} > 0.6$ as the inflection point becomes closer to the nearest brace point. Conversely, when the R_m term is neglected, Eq. 2 provides more accurate estimates, ranging from 0-20% conservative for all practical values of $\rho_{top,base}$. When comparing the results in Fig. 8 with the reverse-curvature cases in Fig. 7 (I-0, E-0, I-1, and E-1), it is shown that the R_m term produces significant errors for nearly linear moment gradients and M_{small}/M_{large} ratios greater than -1/3 (or inflection points within $L_b/3$ of the nearest brace point).

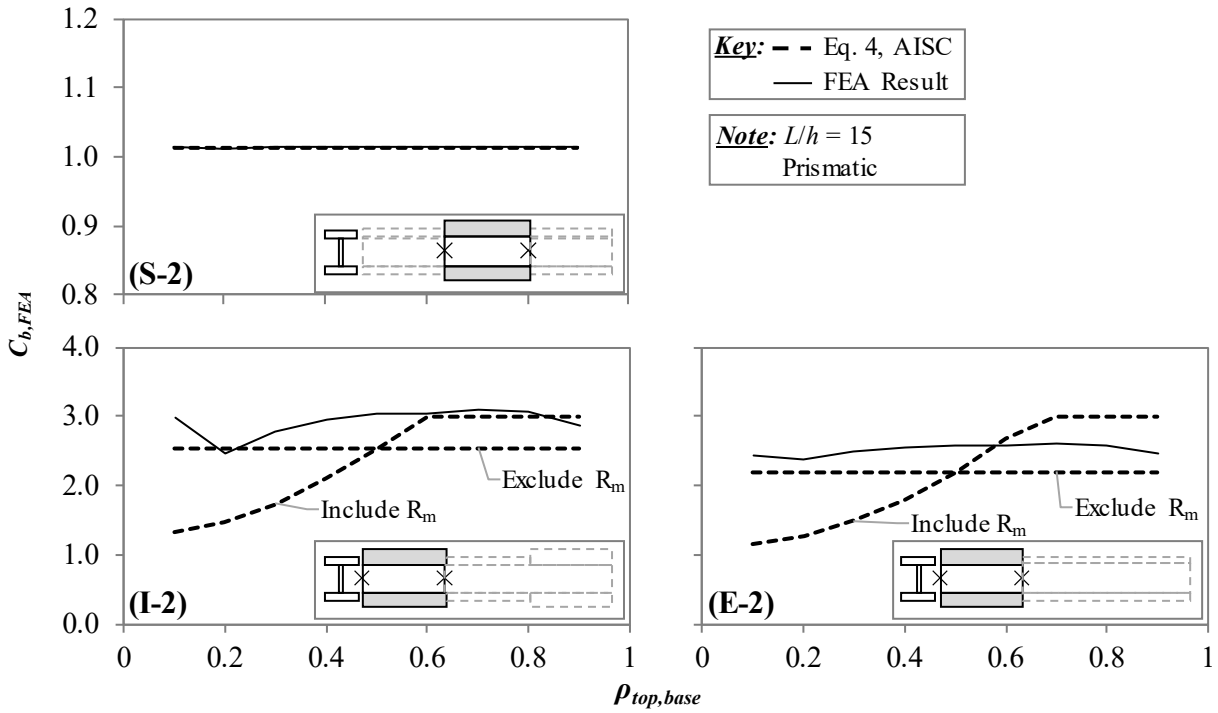

Figure 8: FEA results compared to the AISC approximate solution (Eq. 2) for moment gradient cases S-2, I-2, and E-2.

5. Conclusions and Design Recommendations

Based on the results presented in the preceding section, it is concluded that: (1) the AISC expression for C_b approximates the analytical solutions for nonprismatic girders with reasonable conservatism and (2) the R_m term should be neglected for single-curvature bending and reverse-curvature bending when $M_{small}/M_{large} > -1/3$. For girder sections within practical values of ρ_{top}, these approximate solutions produce estimates on the order of 0-30% conservative.

For singly-symmetric, nonprismatic sections in single- or reverse-curvature, which are common cases in bridge engineering, the approach for C_b is generally unchanged from current AASHTO procedures. The proposed AISC expression (Eq. 2) is calculated in terms of moments instead of stresses and is easier to implement. The equation, which has been shown to provide reasonably estimates of the buckling solution, is to be applied equally to all different cross-sections within a nonprismatic segment. Those individual sections must then be checked against the respective yield moment to ensure the critical limit state is considered.

This work can be further progressed by investigating different bracing schemes, multiple transitions along an unbraced length, and variable transition lengths instead of the fixed $0.3L$ and $0.7L$ used here. In addition, considering increased flange widths within transition regions, load height effects, and variable-depth girders could potentially be explored. It is acknowledged that the AISC moment gradient equation can produce overly conservative estimates for some extreme cases. But given that it is very straightforward to use and has shown to produce reasonably conservative approximations for the most common girder and bracing conditions, the AISC C_b expression is promising for steel bridge applications.

References

Abaqus/CAE (2017). "Abaqus/CAE User's Guide."

American Association of State Highway and Transportation Officials (2017). "LRFD Bridge Design Specifications (8th ed.)". Washington, D.C.

American Institute of Steel Construction (2016). "Specification for Structural Steel Buildings." Chicago, IL

Galambos, T. (1968). "Structural Members and Frames." Prentice Hall. Englewood Cliffs, NJ

Helwig, T., Frank, K., Yura, J. (1997). "Lateral-Torsional Buckling of Singly Symmetric I-Beams." *Journal of Structural Engineering*, 123 (9) 1172-1179.

White, D., Jung, S. (2003). "Simplified Lateral-Torsional Buckling Equations for Singly-Symmetric I-section Members: Structural Engineering, Mechanics and Materials Report No. 24b." Georgia Institute of Technology, School of Civil and Environmental Engineering. Atlanta, GA.

Ziemian, R. (2010). "Stability Design Criteria for Metal Structures: Sixth Edition." John Wiley & Sons, Inc. Hoboken, NJ.